

Process-Based Indicators for Timely Identification of Apricot Frost Disaster on the Warm Temperate Zone, China

Yang Jianying

China Academy of Meteorological Sciences

Zhiguo Huo (✉ huozhiguo_cma@126.com)

China Academy of Meteorological Sciences

Peijuan Wang

China Academy of Meteorological Sciences

Wu Dingrong

China Academy of Meteorological Sciences

Yuping Ma

China Academy of Meteorological Sciences

Research Article

Keywords: Apricot, Frost process, Identification indicator, Monitoring and warning

Posted Date: March 15th, 2021

DOI: <https://doi.org/10.21203/rs.3.rs-268838/v1>

License:  This work is licensed under a Creative Commons Attribution 4.0 International License.

[Read Full License](#)

Process-based indicators for timely identification of apricot frost disaster on the warm temperate zone, China

Jiaying Yang^a, Zhiguo Huo^{a,b}*, Peijuan Wang^a, Dingrong Wu^a, Yuping Ma^a

1. State Key Laboratory of Severe Weather (LASW), Chinese Academy of Meteorological Sciences, Beijing 100081, China;

2. Collaborative Innovation Center of Forecast and Evaluation of Meteorological, Nanjing University of Information Science &

Technology, Nanjing 210044, China

Abstract

Frequent occurrences of extreme cold weather processes create severe agricultural/forest frost events, even given the background of global warming. In the warm temperate zone of China, which is the largest planting area for fresh apricot, late spring frost disaster has become one of the major meteorological hazards during flowering. To prevent cold weather-induced apricot frost events and reduce potential losses in related fruit economic value, it is vital to establish a meteorological indicator for timely and accurate identification of cold weather process-based apricot frost events, to provide support for timely apricot frost monitoring and warning in late spring. In this study, daily minimax temperature (T_{min}) and apricot frost disaster data during flowering were combined to establish meteorological identification indicators of apricot frost based on cold weather processes. A process-based apricot frost model $f(D, T_{cum})$ was firstly constructed, and characteristics of T_{cum} (accumulated harmful temperature) were explored under different D (duration days) based on the representation of historical apricot frost processes. Thresholds for the T_{cum} for apricot frost in 1, 2, 3, 4 and more than 5 days of apricot frost process were determined as -1.51, -2.92, -4.39, -5.84

* Corresponding author at: No. 46, Zhongguancun South Street, Haidian District, Beijing 100081, PR China. Tel.: +86 10 58993238;

E-mail addresses: huozhiguo_cma@126.com(Z. Huo)

21 and -7.31°C , respectively. Validation results by reserved independent disaster samples were
22 generally consistent with the historical records of apricot frost disasters, with 89.00% accuracy for
23 indicator-based identification results. Typical process tracking of the proposed identification
24 indicator to an apricot frost event that occurred in North Hebei during April 3-9, 2018 revealed that
25 the indicator-based identification result basically coincides with the historical disaster record and
26 can reflect more detailed information about the apricot frost process.

27 Key words: Apricot; Frost process; Identification indicator: Monitoring and warning

28 1 Introduction

29 Frost, as a temperature-related meteorological disaster, has been recognized as a
30 major threat to the normal growth and production of agriculture and forest productivity
31 through freeze damage (Vitasse, et al., 2018). As public generally believe that climate
32 change is a scientific conclusion, a decrease in the frequency and intensity of frost
33 events has been speculated with global warming. Paradoxically, as temperatures
34 increase in early spring, perennial crops such as fruit trees gradually become
35 increasingly vulnerable to cold temperatures, because of climate fluctuation that has led
36 to considerable phenological shifts, such as advancing the date of flowering, and
37 accelerating vegetative development, leading to the advancement of frost-sensitive
38 stages due to a warmer winter and spring (Shimono, 2011; Saeidi et al., 2012; Chen et
39 al., 2014; Wang et al., 2018). Frost disaster is widely reported in North American
40 ecosystems (Gu et al., 2008; Augspurger, 2013) and forest and fruit trees in Europe
41 (Yann et al., 2018). Timely monitoring of the occurrence of frost events is of
42 considerable importance for adopting targeted measurements to reduce economic and

43 production losses.

44 Cereals (e.g., maize and wheat) (Wang et al., 2013; Wang et al., 2019) and
45 economic plantings (e.g., beech, apple, coffee and tea) (Susan et al., 2018; Antonio et
46 al., 2019; László et al., 2019) have been shown to be vulnerable to frost, with different
47 performance characteristics and mechanisms in response to frost. For example, serious
48 frost caused by an extreme cold event has been witnessed after an earlier growing
49 season onset, resulting in considerable loss of fruit tree yield and quality (Frederiks et
50 al., 2015; Crimp et al., 2016). Additionally, cold tolerance varies between species.
51 When the low temperature weather continues and frost stress increase, plants are injured
52 irreparably, with destruction in fruit yield and quality, that is, a fruit tree frost event. To
53 trigger a fruit tree frost event, two fundamental factors must be linked: the first is the
54 cold weather event, including the starting/ending time, duration, degrees of cold, etc.
55 The second is the plants' characteristics against cold, which always differs based upon
56 the target fruit tree species and its phenological phase (Yang et al., 2016; Yang et al.,
57 2020).

58 To explore the cold weather conditions that cause a frost event, studies on the frost
59 effect on fruit trees have been primarily focused on environment-controlled
60 experiments (Hatice et al., 2019;), designing specific experiments by controlling cold
61 environment to examine the mechanisms of frost effect and the relationships with yield
62 and quality factors. Through controlled experiments, the impacts of low temperatures
63 on crop or fruit trees can be directly observed and detected, following the strategy of
64 changing one element while others are stably maintained.

65 Largely, attention been focused on the spatiotemporal patterns of meteorological
66 frost and their influences on crops (Xiao et al., 2018) in regional assessment. Long
67 series of historical meteorological and yield data have generally been combined to
68 explore the negative impact of frost on crop and fruit trees, affiliating its spatiotemporal
69 distribution and risk changes. For example, Xiao et al. (2018) analyzed frost risk from
70 a meteorological perspective based on the relationship between meteorological factors
71 and yield changes. Relationships between crop or fruit productivity and low
72 temperature indices can provide basic information on the frequency and magnitude of
73 extremes events and their influence on agricultural or forests, but for timely monitoring
74 or warning, pre- and during- frost damage are of more importance because the
75 occurrence of agro-/forest frost events are always attributed to certain extreme cold
76 processes. So, evaluating the extent of the process event-damage is of more importance.

77 Apricot (*Prunus armeniaca* L.), the naturally dominant fresh apricot tree species
78 of the warm temperate zone in China, has suffered late spring frost on the flowers and
79 unripe fruits in orchards, which can dramatically impact apricot production (Ozkan, et
80 al., 2018), since it negatively affects the biomass, reproduction, fruit growth, and
81 ultimately the yield and fruit quality. In this paper, a process-based apricot frost model
82 is proposed that could provide timely, accurate monitoring and warning of an apricot
83 frost event based on meteorological method throughout the flowering season (from mid-
84 March to late-April), when spring cold occurs in late spring. The main goal is to
85 statistically characterize apricot frost events in the China warm temperate zone and to
86 develop a process-based indicator for timely monitoring and warning of apricot frost

87 disaster, with the ultimate goal of facilitating better orchard management to mitigate
88 the effect of disaster weather.

89 2. Materials and methods

90 2.1 Study area

91 The warm temperate zone of China is a major fresh apricot production area located
92 in Northern China between 24°~42°N and 125°~104°E that includes Hebei, Henan,
93 Shandong, Shanxi, Shaanxi, Beijing, and Tianjin provinces, as well as the areas of east
94 of Lanzhou (Gansu province), south of Shenyang (Liaoning province), South of
95 Ningxia, and northern part of Anhui and Jiangsu provinces (Fig.1). Fresh apricots
96 account for more than 50% of the country's total output in this region (Zhang and Zhang,
97 2003). The unique geographical location makes it vulnerable to the extreme cold surges
98 from eastern Siberia or eastern Mongolia. The cold air goes south via North China,
99 resulting in frost damage in winter and early spring (Ding and Krishnamurti, 1987;
100 Wang, 2018; Ding et al., 2021). Severe cold extremes have been witnessed frequently
101 in this region, resulting in severe damage to the public and the economy in recent
102 decades. For example, during the early spring period in 2018, an extreme cold weather
103 process assaulted the warm temperate zone, with a temperature decrease of more than
104 14 °C. This resulted in huge areas of crops and fruit trees, including apricot, being
105 destroyed, and it caused an economic loss of more than 2 billion dollars (Beijing
106 Climate Center, 2018).

107 2.2 Meteorology and disaster records

108 Datasets including meteorological data and disaster records were used to construct
109 apricot frost samples, facilitating the identification of indicators of apricot frost in the
110 flowering phase in this study. Meteorological data from 150 weather stations were
111 obtained from the National Meteorological Information Centre, China Meteorological
112 Administration (NMIC, CMA), including daily minimum temperature datasets from
113 1981 to 2018. Apricot frost disaster records can be derived in the *China Meteorological*
114 *Disasters Book* (Hebei, Shandong, Henan, Shaanxi, Shanxi, Gansu, Ningxia, Beijing,
115 Tianjin, Jiangsu, Anhui), the *Yearbook of Meteorological Disasters in China*, forest and
116 fruit disasters surveys, county-based disaster records for the fruit industry, and relevant
117 media reports. Apricot frost disaster records include the time, location, and the
118 destruction of apricot flowers covering the period from 1981 to 2018, clearly recorded
119 with the freezing injury time and disaster occurrence areas.

120 2.3 Theoretical model of process-based apricot frost disaster

121 2.3.1 Derivation of apricot frost disaster-causing factors

122 Frost is mainly induced by the cold weather process, which can be derived from:
123 (1) radiation frost, that is surface energy continuously radiates to the atmosphere, during
124 calm winds, clear skies, and a temperature inversion, (2) advection frost, that is cold air
125 advection to a region during moderate-to-high winds, overcast skies, without inversion,
126 and (3) mixed type of both conditions (Wang et al., 2019). The daily minimum
127 temperature, low temperature duration, diurnal temperature range, and accumulated
128 harmful temperature should always be used as disaster-causing factors for the analysis

129 of the three types of frost. The intensity and duration of disaster weather determines
130 whether it can trigger plant injury as was discovered by previous studies (Yang et al.,
131 2016). To demonstrate a frost process on apricot, the frost duration days (D) and the
132 accumulated harmful temperature (T_{cum}) were chose to demonstrate a process-based
133 apricot frost event (as showed in fig. 2), which can be defined as $f(D, T_{cum})$.

134 2.3.2 Derivation of T_{cum} and D

135 Relevant frost trigger thresholds, optimum thermal environment, and the
136 resistance abilities of fruit trees vary with the development phases of the species
137 (Álvaro et al., 2020). Flowering or leaf-out of temperate trees can resist to temperatures
138 between $-8\text{ }^{\circ}\text{C}$ to $-3\text{ }^{\circ}\text{C}$ in experimental work or laboratory studies (László et al.,
139 2019; Hatice et al., 2019). Low temperatures ($-4\text{ }^{\circ}\text{C}$) were applied at full flowering to
140 select optimum apricot genotypes (*Prunus armeniaca* L.) with high resistance to cold in
141 the Cappadocia region (Hatice et al., 2019). However, during clear and windless nights,
142 temperatures measured at 2 m height under the sheltered conditions of a Stevenson
143 screen were established to be 4 to $8\text{ }^{\circ}\text{C}$ degrees higher than those in plant tissues (Ducrey,
144 1998). Temperatures below $0\text{ }^{\circ}\text{C}$, as recorded in a standard weather station, can
145 potentially be used in frost risk analysis on leaves, flowers and young fruits, for the
146 mismatch of temperatures between plant tissues and weather stations (Yann et al., 2018).
147 Commonly, a measured air temperature that is near to $0\text{ }^{\circ}\text{C}$ is considered as a frost
148 trigger threshold for cultivated trees in spring (Ducrey, 1998; Perraudin and Fellay,
149 1975). So, $0\text{ }^{\circ}\text{C}$ was chosen as the temperature potential threshold demonstrated as T_{thr} ,
150 and T_{cum} was used as the ultimately determination to identify an apricot frost.

151 T_{cum} in an apricot frost event was calculated as follows:

$$152 \quad T_{cum} = \sum_{D=1}^j (T_{min} - T_{thr}) \quad (1)$$

153 Here, T_{cum} is the accumulated harmful temperature in the apricot frost event;
154 T_{min} is the daily minimum temperature below T_{thr} . T_{thr} is a threshold temperature,
155 that is 0°C.

156 D is the consecutive days that $T_{min} < T_{thr}$.

157 2.4 Historical apricot frost process representation

158 To represent historical apricot frost processes in this study, times and locations of
159 historical apricot frost disaster records, as well as the daily minimum temperature data,
160 were firstly integrated, and afterwards, D and T_{cum} in the apricot frost process were
161 rechecked and calculated according to formula (1). Extreme low temperature processes
162 causing apricot frost were determined after considering the D in a catchment. We took
163 an apricot frost disaster in early April 1993 in Changzhi county (Shanxi province) as an
164 example. Records describe this apricot frost disaster as, “At the beginning of April 1993,
165 frost weather condition caused apricot, peach and pear petals fell off in Changzhi,
166 Shanxi province”. Daily T_{min} data were extracted from the Changzhi Meteorological
167 Station, with $T_{min} < 0^{\circ}\text{C}$ from April 7th to April 11th, with T_{min} were -1.8, -3.6, -2.2,
168 -5.7 and -2.9 0°C. A historical apricot frost process dataset was built, including D
169 and T_{cum} , that is D (5days) – T_{cum} (-16.2°C).

170 According to this method, 202 samples were represented. We randomly chose 10%
171 of disaster samples for frost identification indicator validation, while 90% of the
172 disaster samples were used for indicator construction. Detailed information of disaster

173 samples for apricot frost are shown in Table 1.

174 2.5 Identification of indicators for an apricot frost

175 Disaster sample sequence distribution fitting, interval estimation, and other
176 methods to acquire the disaster population characteristics and construct agricultural
177 meteorology disaster indicators have been applied and confirmed in the construction of
178 disaster indicators such as agricultural floods (Yang et al., 2016), waterlogging, drought
179 (Wu et al., 2018), and heat damage (Yang et al., 2020). For apricot frost disasters of
180 different duration (in days), the threshold defines, for " $D-T_{cum}$ " combinations, the
181 amount of T_{cum} likely to be triggered for the same D for apricot frost processes. In
182 this study, characterises of disaster population can be attached through the probability
183 density functions or cumulative probabilities of T_{cum} amount in each of the duration
184 datasets. Afterwards, sample coverage rates (SCR) were calculated for different D to
185 identify the most suitable indicators, considering the distribution of disaster samples in
186 the disaster population probabilities.

187 2.5.1 Distribution fitting test of T_{cum} sets

188 Normal, exponential, and uniform distributions are commonly adopted in the
189 expression of disaster characteristics, because of the succinct parameters and simple
190 algorithm. So, we chose the three discrete probability distributions of T_{cum} amount in
191 different D datasets as candidate distributions, representing the historical apricot frost
192 processes.

193 Kolmogorov–Smirnov (K–S) was applied for the goodness of fit testing of T_{cum} .

194 Kolmogorov–Smirnov (K–S) is a test method for comparing a frequency distribution
 195 and a theoretical distribution, or the value distributions of two observations. The null
 196 hypotheses of T_{cum} with a theoretical distribution function in each D were tested with
 197 statistical analyses of maximum difference between the empirical and theoretical
 198 distribution functions (that is, normal, exponential, and uniform). The null hypothesis
 199 is rejected at a given significance level if the test statistic exceeds a critical value (Yang
 200 et al., 2016).

$$201 \quad D_n = \max_{-\infty < x < \infty} |F(x) - \bar{F}(x)| < D_{n,\alpha} \quad (2)$$

202 Here, D_n is a random variable with distribution dependent on n ; $D_{n,\alpha}$ is a
 203 critical value at the level of significance.

204 2.5.2 Identification of the trigger value of T_{cum} for different D

205 The ideal threshold can express most of the disaster population to ensure the
 206 accuracy of identification, while reflecting the concentration of independent samples to
 207 avoid misjudgement in non-disaster populations. The most suitable trigger value or
 208 disaster indicator can be derived from sample coverage rates (SCR). Firstly, inverse
 209 function values of the best fitting of T_{cum} sets were calculated with 5% step size.
 210 Secondly, SCR were calculated under the inverse function values, and we compared
 211 and chose the upper limit with the biggest SCR slope.

$$212 \quad SCR_i = \frac{n_i}{N_i} \quad (3)$$

213 Here, SCR_i is the coverage of disaster samples at the D -th duration days; n_i is
 214 the number of historical disaster samples whose T_{cum} reaches the cumulative
 215 probability of the overall disaster population with 5% step size; N_i is the total

216 historical disaster sample at the D -th duration days.

217 2.6 Validation of process-based apricot frost indicator

218 2.6.1 Reserve independent sample test

219 The rationality of the threshold for apricot frost was verified by comparing the
220 disaster occurrence consistency between the indicator-based results and historical
221 documentation, using the reserved independent apricot frost samples, as showed in part
222 2.4 and Table 1.

223 2.6.2 Typical process tracking

224 An extreme snowfall process and strong wind cooling weather occurred in
225 Northern Hebei in 2018, as a result of which there was frost damage to apricot trees in
226 the northern area. The frost process of apricot in flowering is tracked in this research,
227 through the occurring points and intensity demonstrated in D and T_{cum} , based on the
228 indicators constructed above.

229 3 Results

230 3.1 $f(D, T_{cum})$ characteristics in the historical apricot frost

231 The percentage of duration days for apricot frost process (D) was calculated based
232 on the disaster samples. As shown in Fig.3, the minimum value of D is 1, while the
233 maximum is 6 days in the warm temperate zone of apricot in China. A 3-day process
234 was detected as having the highest possibility of apricot frost, followed by 4-day
235 process, with 23.60 and 23.03% of the frost process continued for 3 days and 4 days,

236 respectively. 7.61% and 6.52 % apricot frost samples lasted for 5 and 6 days,
237 respectively. Considering the frost weather condition and the phenological
238 characteristics that the flowering period of apricot trees generally lasts 7-20 days, 5-
239 and 6-day frost processes will be discussed in a unified manner for the convenience of
240 application. Thus, the characteristics of (D, T_{cum}) were represented as in Fig.4, and the
241 information of T_{cum} in 1, 2, 3, 4 and ≥ 5 days for apricot frost samples are shown in
242 Table 2. The average T_{cum} s were -2.55, -5.53, -11.91, -17.03 and -22.81°C for 1, 2, 3,
243 4 and ≥ 5 days processes, respectively.

244 3.2 Identification of an apricot frost process

245 Results of K-S tests showed that four datasets of T_{cum} series, that is D s 1, 2, 4 and
246 ≥ 5 , followed normal distribution with K-S Sig: 0.189, 0.438, 0.147 and 0.398,
247 respectively (Table 3). One dataset, that is T_{cum} series in 2 days, passed the uniform
248 distribution significance test, with K-S Sig. 0.058, while none passed exponential
249 distribution significance. Comparing the 3-candidate distribution fitting, normal
250 distribution showed better performance than uniform or exponential distributions.
251 Mathematical transformation was taken in T_{cum} in 3-days frost processes, and the final
252 K-S Sig. was 0.078, which passed the significance fitting test.

253 Normal distribution of T_{cum} s at different duration days of apricot frost is shown in
254 Fig.5. The inverse values of normal distribution fitting functions accumulative
255 probability from 70% to 95% are shown as Table 4. The threshold for the apricot frost
256 at each growth stage was identified according to the SCR at 5% cumulative probability
257 step (Fig.6). Comparing the distribution of SCR in 70% to 90%, the slope of SCR was

258 highest from 75% to 80% for 1 to 3 days of apricot frost, while SCR changed gently
259 after 80%, meaning that the disaster samples for 1 to 3 days frost have a high degree of
260 aggregation in range between 75% to 80% disaster population cumulative probability.
261 Considering most independent disaster samples are detected in the inverse value range
262 between 75% and 80% for 1- to 3-days frost processes, and the context of cumulative
263 probability, an inverse value of 80% cumulative probability is more suitable as a
264 potential threshold, for 80% of the disaster population can be detected in such T_{cum}
265 for 1 to 3 days of frost process. Inverse values of T_{cum} at 80% normal cumulative
266 probability were firstly calculated as potential thresholds for 1 day, 2 days, and 3 days
267 of frost processes, respectively. For instance, we took the threshold identification of 1-
268 day frost: the inverse values of T_{cum} were -1.92, -1.74, -1.54, -1.31, -1.02, -0.58 °C
269 for normal distribution fitting function at 0.7 to 0.95 cumulative probability at 5% step,
270 meaning that the inverse values can identify 70%, 75%, 80%, 85%, 90%, and 95% of
271 the disaster population for 1-day apricot frost processes. Considering the independent
272 samples distribution and disaster population characteristics, the inverse value of 80%
273 cumulative probability, that is -1.54 °C, was identified as the threshold for 1-day frost
274 processes.

275 Change of SCR for 4 days and ≥ 5 days of apricot frost processes showed that more
276 independent disaster samples can be detected with inverse values of higher normal
277 cumulative probability (or lower T_{cum}). Looking back at apricot frost processes, we
278 found that frost events can be detected in the preceding three days, meaning that the
279 disaster processes can be timely recognized from the 1-3 days as soon as possible,

280 although the process can persist long, and the continuous accumulation of T_{cum}
281 aggravates the degree of frost damage. For 4 days and ≥ 5 days of frost processes, the
282 identification thresholds were firstly constructed by the inverse value of 80%
283 cumulative probability, and then modified according to the results of thresholds of 1-
284 to 3-days processes. For instance, we took the threshold identification of 4 days frost:
285 the inverse value of 80% cumulative probability of T_{cum} in 4 days of apricot frost
286 processes was -7.21°C , which is lower than 4 times of 1 day frost threshold (-1.51°C),
287 2 times of 2 days frost threshold (-2.92°C), and the sum of thresholds for 1 day and 3
288 days processes (-1.51 and -4.39°C). The minimum value of the above was taken as the
289 threshold for 4 days of frost processes, that is, -5.84°C

290 On that basis, thresholds for the T_{cum} for apricot frost in 1, 2, 3, 4 and more than
291 5 days of apricot frost processes were determined, and indicators of apricot frost
292 processes and their activity in disaster samples identification are shown in Table 5. The
293 totally consistent ratio was more than 80% for disaster samples identification.

294 3.3 Validation

295 3.3.1 Validation of reserved independent samples

296 Eighteen random historical apricot frost samples were independently selected to
297 validate the applicability of the proposed apricot frost indicators. Table 6 shows the
298 validation results of the reserved independent samples according to the apricot frost
299 indicator constructed previously. All samples of 1-day, 2-days and more than 5-days
300 frost processes can be identified by the indicators, and the coincidence rate of the frost

301 indicators-based is 100%. One sample in 3 days and 4 days of apricot frost processes
302 failed in the indicator-based identification, with frost indicator accuracies of 75% and
303 80% for 3-days and 4-days apricot frost processes, respectively. Overall, the results
304 calculated by the frost indicators were generally consistent with disaster records in
305 historical documents, with 89.00% of indicator-based results completely consistent
306 with historical records, indicating that the apricot frost indicators can reasonably reflect
307 actual apricot frost events in the study area.

308 3.3.2 Typical process tracking

309 In early spring 2018, a frost event spread from north to south across the warm
310 temperate zone, with a rare snow fall process and strong wind cooling weather. Part of
311 the north region had a minimum temperature below 0 °C (Zhao et al., 2020). Extremely
312 serious destruction of apricot trees was recorded in North Hebei province (located in
313 the north part of the warm temperate zone) because of the frost event. T_{min} of April
314 2018 were extracted from 8 stations in North Hebei, and the average T_{min} were below
315 0° C from April 3th to 9th (Fig. 7). Based on the indicator constructed previously,
316 apricot frost events according the 8 stations were identified daily in North Hebei, as
317 showed in Fig.8. Two stations, accounting for 25% stations, detected suffered from
318 apricot frost in 3th April. Apricot frost developed in April 4th, with 6 stations identifying
319 apricot frost, and this lasted through April 5th and 6th. To April 7^h, all stations were
320 identified suffer from apricot frost. The frost process alleviated gradually from 8th
321 onward, with 88% (7 stations) and 38% (3 stations) detecting apricot frost.

322 4 Discuss

323 4.1 Rationality of theory and method

324 The formation of crop frost is governed by the interacting effects of climatic
325 conditions, topography, soil structure, frost tolerance of crop species, and field/orchard
326 management, among which, weather conditions are the most important frost trigger
327 factor for causing a disaster. To investigate regional frost on crop or fruit trees, yield
328 loss and the amount of temperature-related indexes were quantitatively combined, no
329 matter whether the temperature-related indexes are based on meteorological data or
330 remote sensing (Tao et al., 2017; Xiao et al., 2018). Among them, meteorological based
331 methods are recognized as the most convenient monitoring and are uniquely effective
332 early warning tools (Shi et al., 2020). To date, most studies on forest and fruit frost have
333 focused on the analysis of temperature conditions based on various
334 agricultural/meteorology index calculations during the growing stages (Yang et al.,
335 2020). Previous indicators of crop frost (such as accumulated frost days or accumulated
336 frost-degree days) (Xiao et al., 2018) could represent frost stress or characteristics in
337 crop planting seasons under climate change, whereas the crop/fruit damage due to frost
338 in each growth stage could be assessed based on the frost indicators, and the unique
339 effects of an apricot frost event on crop damage can be predicted in each growth stage
340 of the apricot tree based on the indicator constructed.

341 It is accepted that the occurrence of frost can be triggered by a single threshold,
342 what has demonstrated by previous studies on frost (Snyder et al., 2000; Simões et al.,

2015). For example, 285.5 K was recognized a damage indicator for plants in the tropics (Snyder et al., 2000). However, the extent of crop damage is strongly related to the plant's hardiness and the development of low weather processes. $f(D, T_{cum})$ was adopt to demonstrate process-based apricot frost event, for D is the duration of a frost event and T_{cum} is the intensity of the frost process. The construction process of apricot frost including D and T_{cum} is mainly based on the historical disaster representation and re-analysis in stations. The disaster samples cover the spatial region of the study area and confirmed with long series sequence, which is more vital in the representation of T_{cum} s in D s. Statistical analysis, such as the optimal distribution fitting test, probability inverse function, etc., are methods for retracing the occurrence and development processes of the apricot frost in North temperate zone, and the methods of identification of an apricot frost event are both scientific and regionally applicative.

4.2 Utilization of apricot frost indicators

The effect of frost on fruit yield and quality is a complex process and is variable, as temperature affects so many biological processes in plants, with different species in different phenological phases each having different responses. Apricot has been recognized as a species that is sensitive to cold weather when flower buds have fulfilled the endodormancy with the beginning of active growth, and flower destruction occurs as a result of frost disaster (Hatice et al., 2019). When the low temperature weather continues and frost stress increases, flowers are injured irreparably with flower shedding, leading to an apricot frost event. The indicators identified in our study demonstrate how low temperature conditions accumulate to frost disaster weather for

365 apricot production. The use of the apricot frost indicators can serve as a direct
366 meteorological method to assist in the identification of apricot frost events or processes.

367 Nowadays, operational numerical weather prediction models provide long-term
368 and short-term effective weather forecasts, which help guide the identification of
369 extreme weather phenomena based on space regions and time scales (Susan et al., 2020).
370 The process-based threshold in the identification of apricot frost is operational for its
371 frost forecasting and warning under the given weather forecast productions. More
372 information and measures for apricot frost prevention and mitigation can be
373 implemented according to the indicator-based calculations and results, and these can
374 inform discussions of how to face an apricot frost disaster with the development of
375 weather warning and forecasts.

376 4.3 Uncertainties and limitations

377 Apricot frost occurrence depends on the climatic conditions, species and stand
378 ages. For example, the relationship between altitude and frost occurrence has been
379 found in experiments (Laughlin, 1982; Laughlin and Kalma, 1987; Susan et al., 2018
380 and 2020), that daily T_{min} was lower at higher altitudes in the absence of absorbed
381 ground heat and thinner air. Apricot trees planted in the northward of a hill are likely to
382 experience more harmful cold accumulation than their counterparts southward (Bao,
383 2011). Eastern slope has been shown to have a higher frequency of frost occurrence
384 than western, for the prolonged cooling hours due to early sunset on the eastern slopes
385 and late sunset on the western slopes lead to heat retention on the ground, which is
386 released at night (Susan et al., 2018). In addition, the degree of cold environment

387 exposure in the context of climate change affects apricots' ability to resist frost. Plants
388 frequently exposed to cold conditions may have evolved a greater capacity to conduct
389 a life in such circumstance or to adapt to frost stress (Hatice et al., 2019). For example,
390 frost stress has increased the frost resistance of apricot in Taihang Mountain (including
391 West Shanxi, North Hebei), for meteorological cold weather in such areas has recurred
392 more frequently than in the warm plain in North China. Therefore, it is necessary to
393 continuously optimize and revise the apricot frost trigger thresholds in specific areas
394 according to factors such as soil, terrain, orchard management, and frost resistance
395 abilities. Overall, the apricot frost indicators constructed in this paper is universal in the
396 main apricot-producing areas in the warm temperate zone in China, and they can
397 provide a basis for targeted apricot frost monitoring and warning.

398 Owing to the complicated interacting effects of external factors, such as weather
399 conditions, water and fertilizer conditions, and orchard management, on perennial fruit
400 trees, it is very difficult to accurately predict loss in quality and yield, that can be
401 attributed solely to frost processes. Additionally, the impact of frost on trees is the result
402 of the interaction between the timing of the event, i.e., full winter vs. active growing
403 season, the low temperature weather processes, and phenological plant status (Marco et
404 al., 2018; Yann et al., 2018; Emilia et al., 2019). Data of apricot phenology, especially
405 the flowering data, is an important factor with regard to frost damage, which is outside
406 of this study's scope. Under global warming, earlier leaf unfolding and flowering for
407 perennial trees has been confirmed by biological observation simulation, as a response
408 to a warmer winter. Obviously the most effective and reliable method to resist late

409 spring frosts in apricots, thus avoiding frost damage, is late flowering (Hatice et al.,
410 2019). Development of cold weather-resistant species in winter and spring is another
411 strategy to prevent frost damage (Hatice et al., 2019).

412 5 Conclusion

413 Cold extremes are unavoidable, but the lessons learned from past experience can
414 be used to reduce the damage they inflict. In this study, a process-based apricot frost
415 model $f(D, T_{cum})$ was firstly constructed for the purposes of timely identification of
416 apricot frost events caused by single cold weather processes on the warm temperate
417 zone of China. Characteristics of T_{cum} were explored under different D based on the
418 representation of historical apricot frost processes. Thresholds for the T_{cum} for apricot
419 frost in 1, 2, 3, 4 and more than 5 days of apricot frost processes were determined as -
420 1.51, -2.92, -4.39, -5.84 and -7.31°C, respectively.

421 Given the intensification of climate extremes, improving and innovating apricot
422 frost management measures based on such process-based identification indicators is
423 essential to reduce agro-forest losses associated with frost disasters of apricot in the
424 warm temperate zone. Our findings have important implications for government,
425 orchard farmers, and agricultural insurance to take measures for apricot frost prevention
426 and mitigation. With the continuous improvement of yield and quality data and the
427 supplementation of disaster documents, as well as geological, topographical, and
428 orchard managements, apricot frost trigger thresholds will be continuously optimized
429 and revised in specific areas. Additionally, threshold-based classification of disaster
430 evaluation level needs to be elaborated and enhanced, thereby creating a complete

431 assessment of apricot frost risk in the main planting area of the warm temperate zone.

432 Acknowledgements

433 We gratefully acknowledge the anonymous reviewers for their valuable comments
434 on the manuscript.

435 Conflict of interest

436 The authors declare that they have no conflict of interests.

437 Funding Statement

438 This work is financially supported by National Key R&D Program of China
439 (2018YFC1505605, 2017YFC1502801), and the Basic Research Funds-regular at the
440 Chinese Academy of Meteorological Sciences (2020Z005).

441 Author information

442 Affiliations

443 1. State Key Laboratory of Severe Weather (LASW), Chinese Academy of
444 Meteorological Sciences, Beijing 100081, China

445 Jianying Yang, Zhiguo Huo, Peijuan Wang, Dingrong Wu, Yuping Ma

446 2. Collaborative Innovation Center of Forecast and Evaluation of Meteorological,
447 Nanjing University of Information Science & Technology, Nanjing 210044, China

448 Zhiguo Huo

449 Contributions

450 Jianying Yang: Writing - review & editing, Methodology.

451 Zhiguo Huo: Supervision.

452 Peijuan Wang: Conceptualization.

453 Dingrong Wu: Software.

454 Yuping Ma: Investigation, Data curation.

455 Corresponding author

456 Correspondence to Zhiguo Huo.

457 Availability of data and material

458 The datasets generated during and/or analysed during the current
459 study are available from the corresponding author on reasonable request.

460 Code availability

461 Not applicable.

462 Ethics approval

463 Not applicable.

464 Consent to participate

465 The authors express their consent to participate for research and review.

466 Consent for publication

467 The authors express their consent for publication of research work.

468

469 Reference:

- 470 Álvaro, R.C., Cristina, G., Jesús, R.C., Ramón, P., Guillermo, G., Gordaliza, J., Julio,
471 C., Fernando, M., Luis, G., 2020. Differential response of oak and beech to late
472 frost damage: an integrated analysis from organ to forest. *Agricultural and Forest
473 Meteorology*. 108243.
- 474 Antonio Gazol, J. Julio Camarero, Michele, C., Martín, L., Edurne, M.C., Xaver, S.M.,
475 2019. Summer drought and spring frost, but not their interaction, constrain
476 European beech and Silver fir growth in their southern distribution limits.
477 *Agricultural and Forest Meteorology*. 278, 107695.
- 478 Augspurger, C.K., 2013. Reconstructing patterns of temperature, phenology, and frost
479 damage over 124 years: spring damage risk is increasing. *Ecology*. 94, 41–50.
- 480 Bao, F. P., 2011. *Selected Papers of Fu Baopu*. Beijing: Meteorological Press. (In
481 Chinese)
- 482 Beijing Climate Center, 2018. *Monthly Climate Impact Assessment Report in China*.
483 https://cmdp.ncc-cma.net/influ/moni_china.php (accessed 14 March 2020).
- 484 Chen, L.J., Xiang, H.Z., Miao, Y., Zhang, L., Guo, Z.F., Zhao, X.H., Lin, J.W., Li, T.L.,
485 2014. An overview of cold resistance in plants. *J. Agron. Crop Sci.* 200, 237–245.
- 486 Crimp, S.J., Zheng, B.Y., Khimashia, N., Gobbett, D.L., Chapman, S., Howden, M.,
487 Nicholls, N., 2016. Recent changes in southern Australian frost occurrence:
488 implications for wheat production risk. *Crop Pasture Sci.* 67, 801–811.
- 489 Ding, T., Gao, H., Li, X., 2021. Increasing occurrence of extreme cold surges in North
490 China during the recent global warming slowdown and the possible linkage to the

491 extreme pressure rises over Siberia. *Atmospheric Research*, 248, 105198.

492 Ding, Y.H., Krishnamurti, T.N., 1987. Heat budget of the Siberian high and the winter
493 monsoon. *Mon. Weather Rev.* 115, 2428–2449.

494 Ducrey, M., 1998. Aspects écophysologiques de la réponse et de l'adaptation des sapins
495 méditerranéens aux extrêmes climatiques: gelées printanières et sécheresse
496 estivale.

497 Emilia, A., Luigi, S., Gaspare, C., Giovanni, B., Guido, D.U., Salvatore, F.b., Angelo,
498 R., Sergio, R., Antonio, S., Giulliano, B., 2019. Canopy damage by spring frost in
499 European beech along the Apennines: effect of latitude, altitude and aspect",
500 *Remote Sensing of Environment*, 225, 431–440.

501 Frederiks, T.M., Christopher, J.T., Sutherland, M.W., Borrell, A.K., 2015. Post-
502 heademergence frost in wheat and barley: defining the problem, assessing the
503 damage, and identifying resistance. *J. Exp. Bot.* 66, 3487–3498.

504 Gu, L., Hanson, P.J., Post, W.M., Kaiser, D.P., Yang, B., Nemani, R., Pallardy, S.G.,
505 Meyers, T., 2008. The 2007 eastern US spring freeze: increased cold damage in a
506 warming world? *AIBS Bull.* 58, 253–262.

507 Hatice, D., Veli, E., Ali, K., Said, E.D., Rabia, A.D., Zahide, K., Cemil, E., Tahir, M.,
508 Melike, B., 2019. Spring late frost resistance of selected wild apricot genotypes
509 (*Prunus armeniaca* L.) from Cappadocia region, Turkey. *Scientia Horticulturae*.
510 246, 347–353.

511 Hatice, D., Veli, E., Ali, K., Said, E.D., Rabia, A. D., Zahide, K., Cemil, E., Tahir, M.,
512 M, B., 2019. Spring late frost resistance of selected wild apricot genotypes (*Prunus*

513 armeniaca L.) from Cappadocia region, Turkey, *Scientia Horticulturae*. 246, 347–
514 353.

515 László, S., Zsuzsanna, G., Magdolna, T., 2019. Frost hardiness of apple (*Malus X*
516 *domestica*) flowers in different phenological phases, *Scientia Horticulturae*. 253,
517 309–315.

518 Laughlin, G.P., 1982. Minimum temperature and lapse rate in complex terrain:
519 influencing factors and prediction. *Theor. Appl. Climatol.* 30 (1), 141–152.

520 Laughlin, G.P., Kalma, J.D., 1987. Frost hazard assessment from local weather and
521 terrain data. *Gricult. For. Meteorol.* 40 (1), 1–16

522 Marco, B., Sofia, B., Francesco, M., Giorgio, M., 2018. Assessing spring frost effects
523 on beech forests in Central Apennines from remotely-sensed data. *Agricultural and*
524 *Forest Meteorology*. 248, 240–250.

525 Ozkan, K., Cafer, K., Tevhit, G., 2018. An exothermic process involved in the late
526 spring frost injury to flower buds of some apricot cultivars (*Prunus armenica* L.).
527 *Scientia Horticulturae*. 241, 322–328.

528 Perraudin, G., Fellay, D., 1975. Les moyens de lutte. La lutte contre le gel. *Revue Suisse*
529 *de Vitic. Arboric. Hortic.* 7, 31–54.

530 Saeidi, M., Eliasi, P., Abdoly, M., Sasani, S., 2012. Freezing tolerance of wheat
531 cultivars at the early growing season after winter. *Afr. J. Biotechnol.* 11, 4045–
532 4052.

533 Shi, J., Cui, L., Tian, Zhan., 2020. Spatial and temporal distribution and trend in flood
534 and drought disasters in East China. *Environmental Research*. 185, 109406.

535 Shimono, H., 2011. Earlier rice phenology as a result of climate change can increase
536 the risk of cold damage during reproductive growth in northern Japan. *Agric.*
537 *Ecosyst. Environ.* 144, 201–207.

538 Simões, D.S., Fontana, D.C., Vicari, M.B., 2015. Use of LST images from
539 MODIS/AQUA sensor as an indication of frost occurrence in RS. *Rev. Bras. Eng.*
540 *Agrícola e Ambient.* 19 (10), 920–925.

541 Snyder, R.L., 2000. Principles of Frost Protection. Published 2000. (Accessed 3 January
542 2017). [http://biomet.ucdavis.edu/frostprotection/Principles%20](http://biomet.ucdavis.edu/frostprotection/Principles%20of%20Frost%20Protection/FP005.html)
543 [of %20Frost%20Protection/FP005.html](http://biomet.ucdavis.edu/frostprotection/Principles%20of%20Frost%20Protection/FP005.html).

544 Susan, M., Kotikot, A.F., Robert, E., Griffin, J.N., Jonathan, L.C., Robinson, M., Absae,
545 S., Emily, A., Ashutosh, L., Daniel, E.I., 2020. Statistical characterization of frost
546 zones: Case of tea freeze damage in the Kenyan highlands. *Int J Appl Earth Obs*
547 *Geoinformation.* 84, 101971.

548 Susan, M., Kotikota, A. F., Robert, E.G., Absae, S., James, N., Robinson, M., Ashutosh,
549 L., Daniel, E. I., 2018. Mapping threats to agriculture in East Africa: Performance
550 of MODIS derived LST for frost identification in Kenya’s tea plantations. *Int. J.*
551 *Appl. Earth Obs. Geoinformation.* 72 , 131–139.

552 Tao, F.L., Xiao, D.P., Zhang, S., Zhang, Z., Rotter, R.P., 2017. Wheat yield benefited
553 from increases in minimum temperature in the Huang-Huai-Hai Plain of China in
554 the past three decades. *Agric. For. Meteorol.* 239, 1–14.

555 Vitasse, Y., Schneider, L., Rixen, C., Christen, D., Rebetez, M., 2018. Increase in the
556 risk of exposure of forest and fruit trees to spring frosts at higher elevations in

557 Switzerland over the last four decades. *Agricultural and Forest Meteorology*, 248,
558 60–69.

559 Wang, P. J., Huo, Z.G., Yang, J.Y., Wu, X., 2019. Indicators of chilling damage for
560 spring maize based on heat index in Northeast China. *Journal of Applied
561 Meteorological Science*, 30(1):13-24. (Chinese with English abstract)

562 Wang, H.F., Guo, W., Wang, J.H., Huang, W.J., Gu, X.H., Dong, Y.Y., Xu, X.G., 2013.
563 Exploring the feasibility of winter wheat freeze injury by integrating grey system
564 model with RS and GIS. *J. Integr. Agric.* 12, 1162–1172.

565 Wang, Z.B., Chen, J., Tong, W.J., Xu, C.C., Chen, F., 2018. Impacts of climate change
566 and varietal replacement on winter wheat phenology in the North China plain. *Int.
567 J. Plant Prod.* 12, 251–263.

568 Wang, Z.M., 2018. Tracks and Characteristics Analysis of Strong Cold Air Invading
569 Northern China during Winter Half Year. Doctoral dissertation. Nanjing
570 University of Information Science & Technology, Nanjing.

571 Wu, X., Wang, P.J., Huo, Z.G., Wu, D.R., Yang, J.Y., 2018. Crop Drought
572 Identification Index for winter wheat based on evapotranspiration in the Huang-
573 Huai-Hai Plain, China. *Agric. Ecosyst. Environ.* 263, 18–30.

574 Xiao, L.J., Liu, L.L., Asseng, S., Xia, Y.M., Tang, L., Liu, B., Cao, W.X., Zhu, Y.,
575 2018. Estimating spring frost and its impact on yield across winter wheat in China.
576 *Agric.For. Meteorol.* 260, 154–164.

577 Yang, J.Y., Huo, Z.G., Li, X.X., Wang, P.J., Wu, D.R., 2020. Hot weather event-based
578 characteristics of double-early rice heat risk: A study of Jiangxi province, South

579 China. *Ecological Indicators*, 113, 106148.

580 Yang, J.Y., Huo, Z.G., Wu, L., Wang, T.Y., Zhang, G.X., 2016. Indicator-based
581 evaluation of spatiotemporal characteristics of rice flood in Southwest China.
582 *Agric. Ecosyst. Environ.* 230, 221–230.

583 Yann, V., Léonard, S., Christian, R., Danilo, C., Martine, R., 2018. Increase in the risk
584 of exposure of forest and fruit trees to spring frosts at higher elevations in
585 Switzerland over the last four decades. *Agricultural and Forest Meteorology*. 248,
586 60–69.

587 Yann, V., Léonard, S., Christian, R., Danilo, C., Martine, R., 2018. Increase in the risk
588 of exposure of forest and fruit trees to spring frosts at higher elevations in
589 Switzerland over the last four decades. *Agricultural and Forest Meteorology*. 248,
590 60–69

591 Zhang, J.Y., Zhang, Z., 2003. *Chinese Fruit Tree (Apricot)*. China Forestry Publish:
592 Beijing.

593 Zhao, L.C., Li, Q. Z., Zhang, Y., Wang, H.Y., Du, X., 2020. Normalized NDVI valley
594 area index (NNVAI)-based framework for quantitative and timely monitoring of
595 winter wheat frost damage on the Huang-Huai-Hai Plain, China. *Agriculture,
596 Ecosystems and Environment*. 292, 106793.

597

Figures

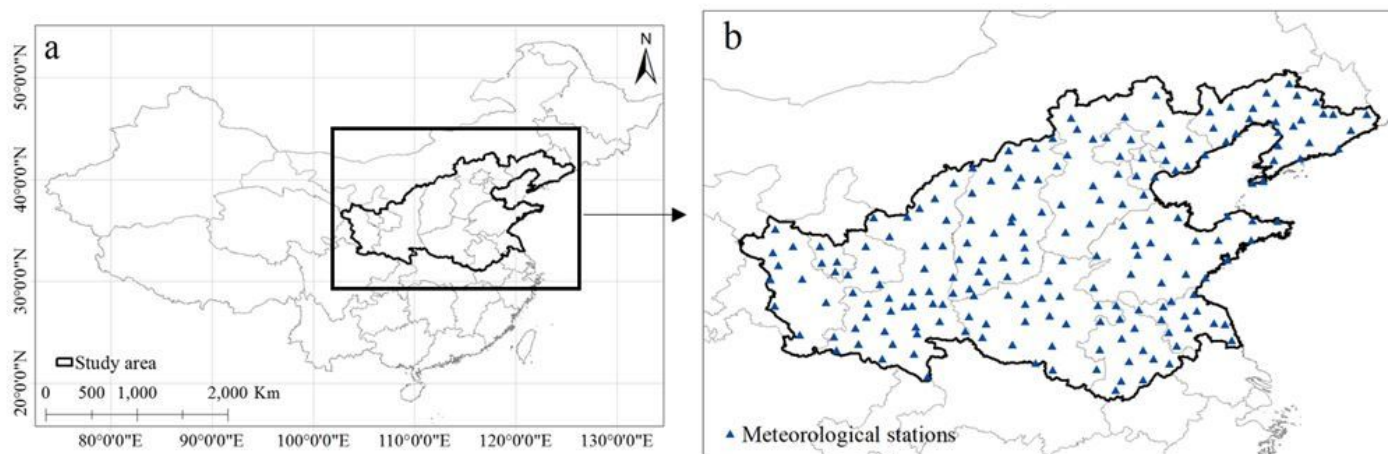


Figure 1

The inset map shows the location of the warm temperate zone of apricot cultivation and meteorological stations. Note: The designations employed and the presentation of the material on this map do not imply the expression of any opinion whatsoever on the part of Research Square concerning the legal status of any country, territory, city or area or of its authorities, or concerning the delimitation of its frontiers or boundaries. This map has been provided by the authors.

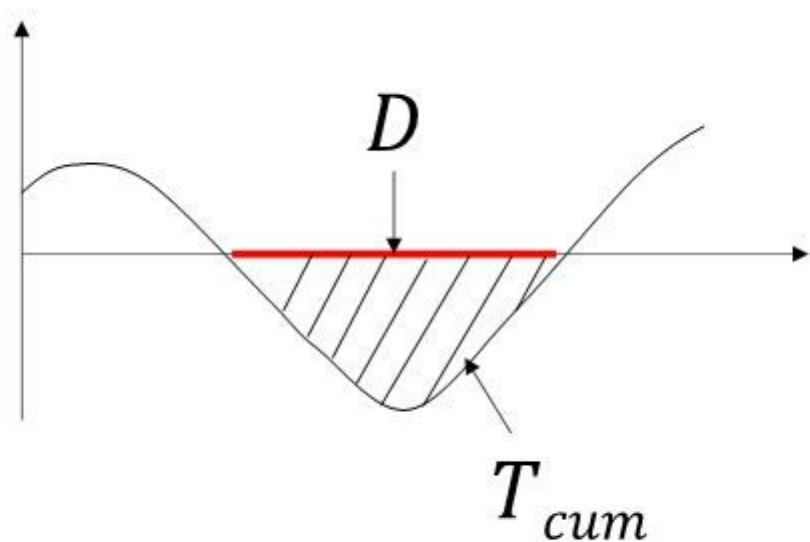


Figure 2

The theoretical diagram of the apricot frost disaster-causing factors for a process-based apricot frost event.

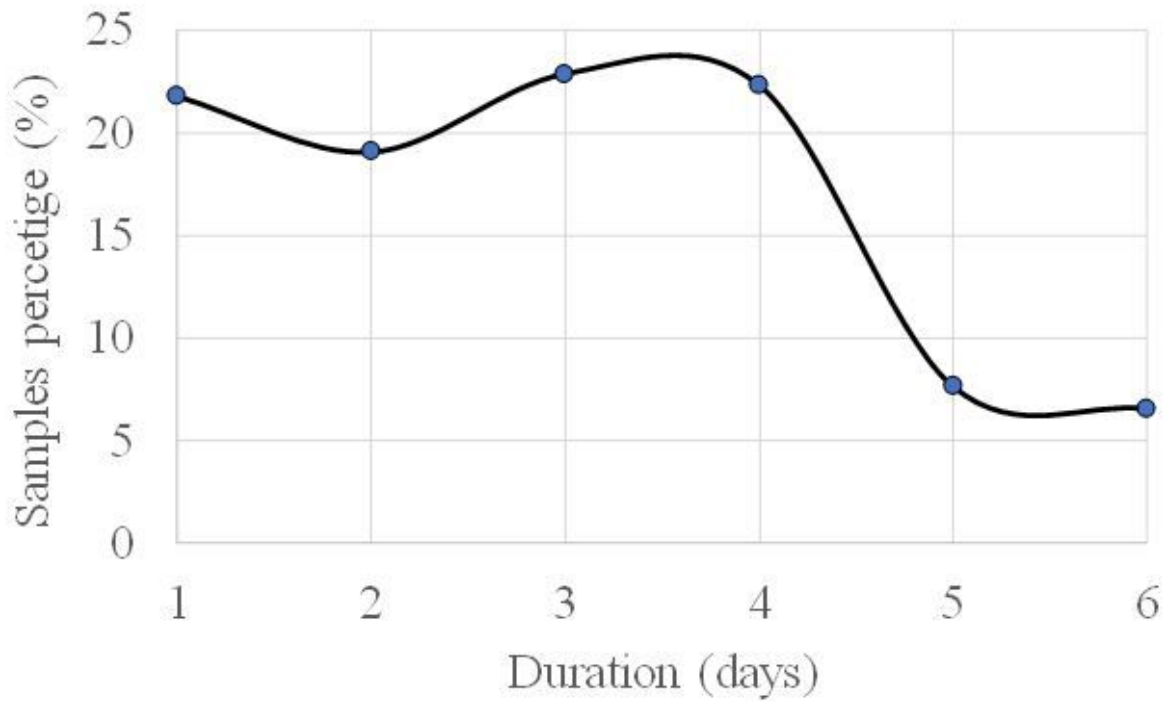


Figure 3

Duration frequency of D in historical apricot frost samples.

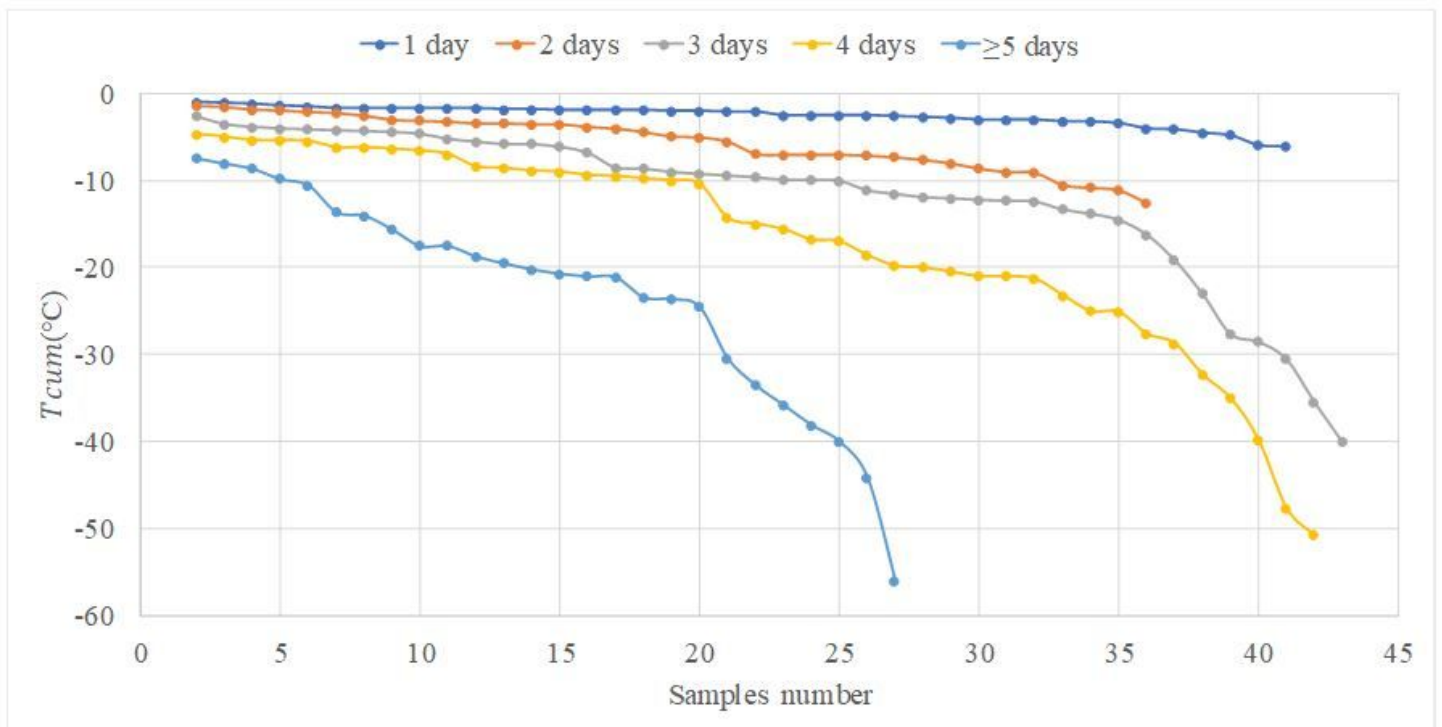
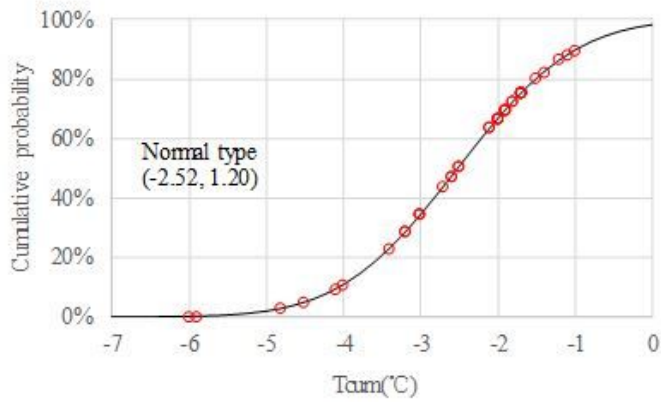
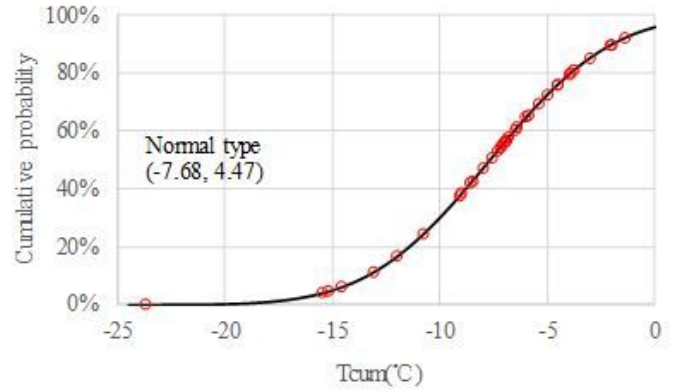


Figure 4

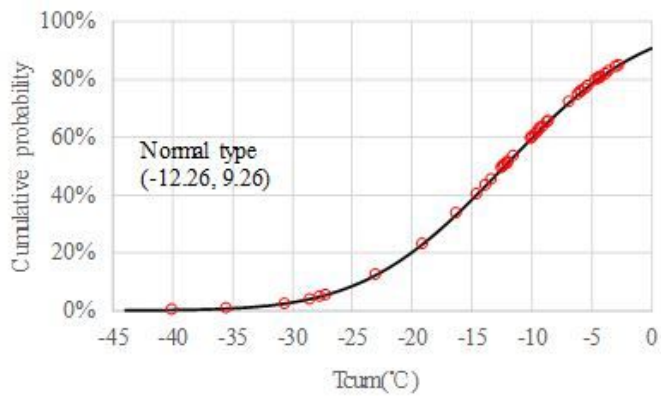
Representation of T_{cum} characteristics for different D



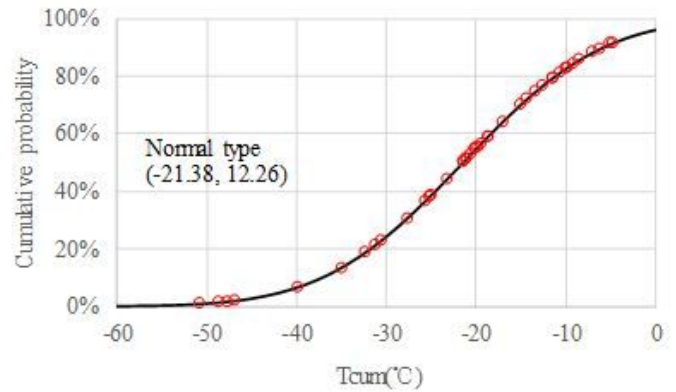
a



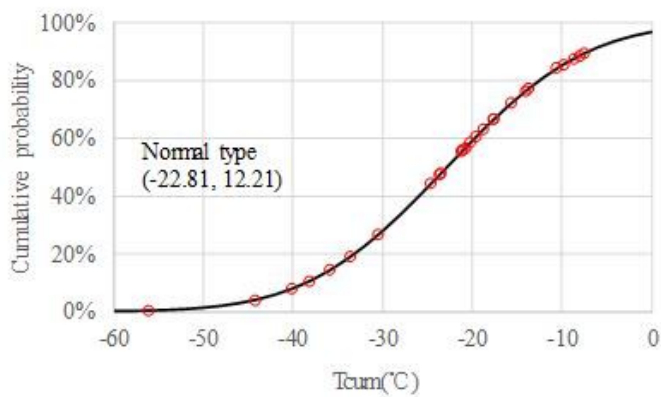
b



c



d



e

Figure 5

Normal distribution of T_{cums} for different D s. Notes: a is normal distribution of T_{cums} in $D=1$ day; b is normal distribution of T_{cums} in $D=2$ days; c is normal distribution of T_{cums} in $D=3$ days; d is normal distribution of T_{cums} in $D=4$ days; e is normal distribution of T_{cums} in $D \geq 5$ days.

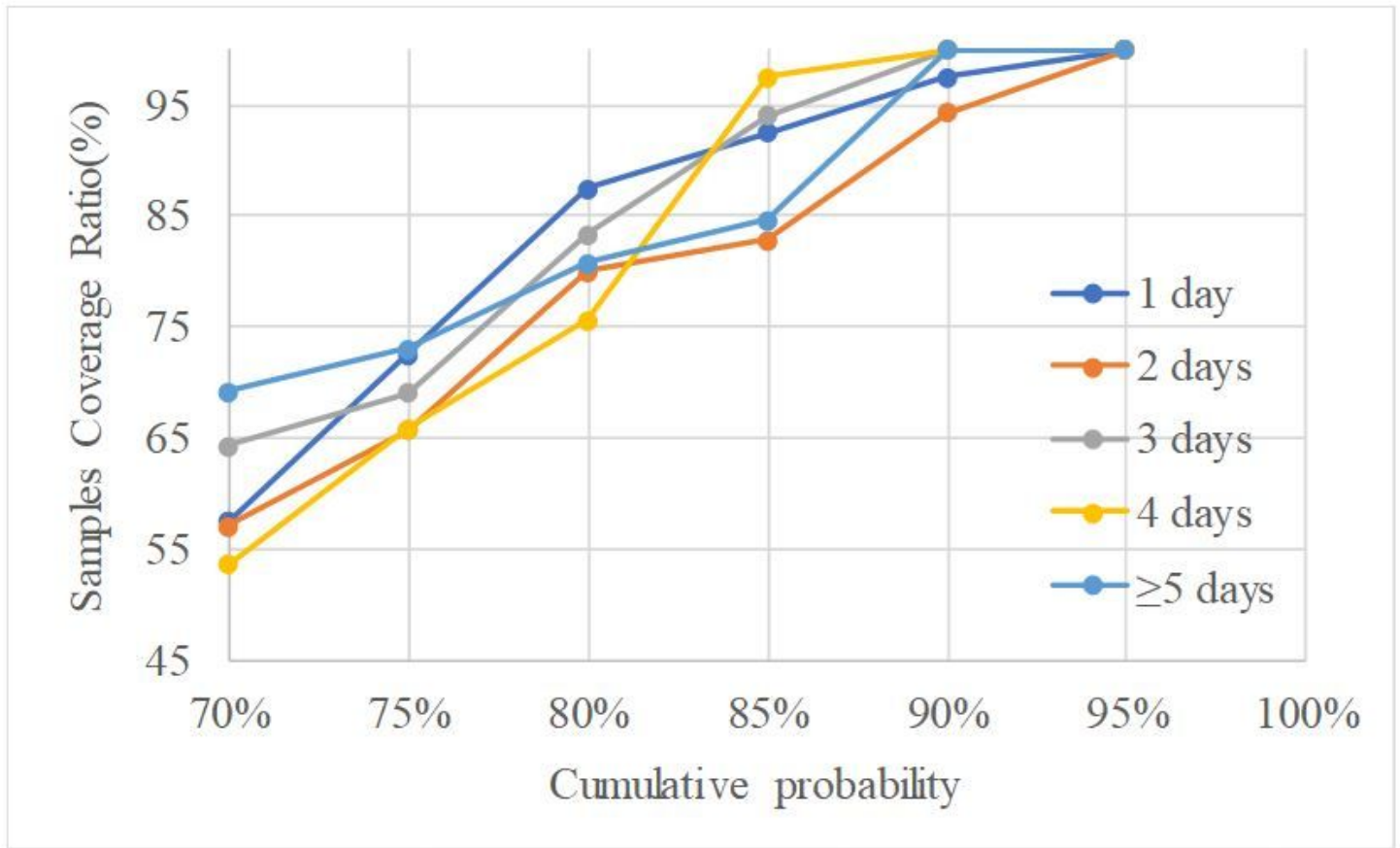


Figure 6

SCR distribution under different cumulative probabilities of best fitting of T_{cum}

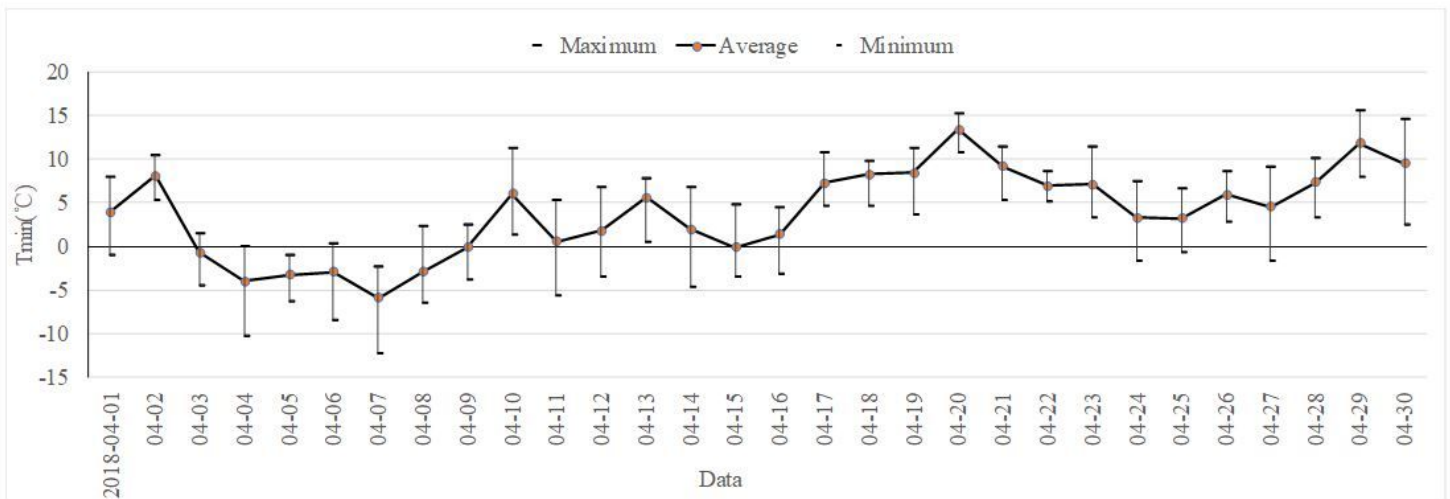


Figure 7

Daily change of regional T_{min} in April 2008.

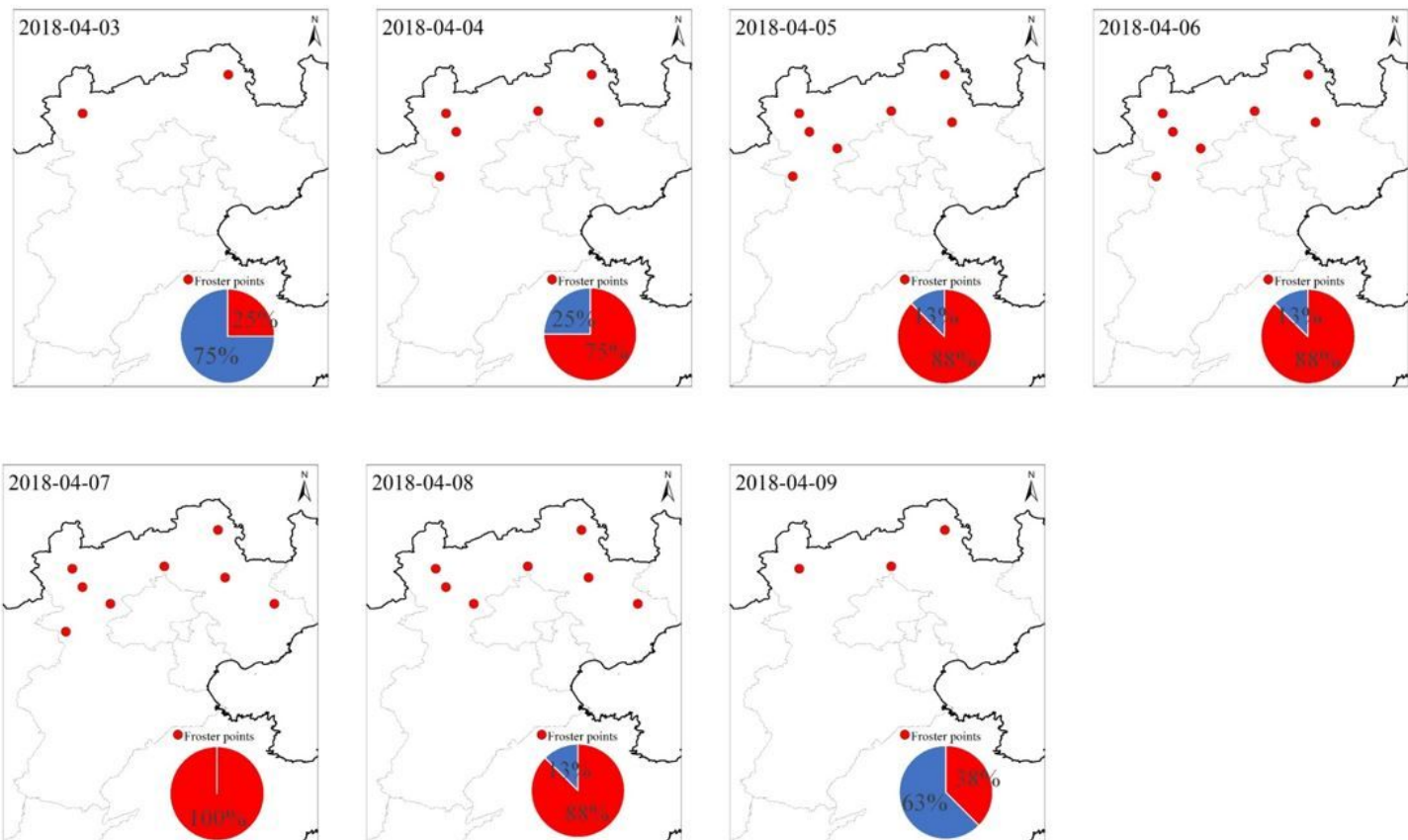


Figure 8

Typical apricot frost process tracking in April 3th-9th, 2008. The red points were identified apricot frost based on the indicator. Note: The designations employed and the presentation of the material on this map do not imply the expression of any opinion whatsoever on the part of Research Square concerning the legal status of any country, territory, city or area or of its authorities, or concerning the delimitation of its frontiers or boundaries. This map has been provided by the authors.